Published for SISSA by Springer

Received: *March 21, 2024*
Revised: *April 9, 2024*
Accepted: *April 24, 2024*
Published: *May 13, 2024*

# Search for $\Delta S = 2$ nonleptonic hyperon decays $\Omega^- \to \Sigma^0\pi^-$ and $\Omega^- \to nK^-$

**The BESIII collaboration**

*E-mail:* besiii-publications@ihep.ac.cn

Abstract: Using $(27.12 \pm 0.14) \times 10^8$ $\psi(3686)$ events collected by the BESIII detector at the center-of-mass energy of $\sqrt{s} = 3.686\,\text{GeV}$, we search for the first time for two nonleptonic hyperon decays that change strangeness by two units, $\Omega^- \to \Sigma^0\pi^-$ and $\Omega^- \to nK^-$. No significant signal is observed. The upper limits on their decay branching fractions are determined to be $\mathcal{B}(\Omega^- \to \Sigma^0\pi^-) < 5.4 \times 10^{-4}$ and $\mathcal{B}(\Omega^- \to nK^-) < 2.4 \times 10^{-4}$ at the 90% confidence level.

Keywords: Beyond Standard Model, $e^+$-$e^-$ Experiments, Rare Decay

ArXiv ePrint: 2403.13437



https://doi.org/10.1007/JHEP05(2024)141

## Contents



## 1 Introduction

In the Standard Model (SM), nonleptonic hyperon decays involving a change in strangeness by two units ($\Delta S = 2$) are highly suppressed. The branching fractions (BFs) of these decays in the SM are at the level of $10^{-17}$–$10^{-12}$ [1], which is far below the existing experimental limits. Currently, there are only two $\Delta S = 2$ processes observed, $K^0 - \bar{K}^0$ mixing and $B_s - \bar{B}_s$ mixing. The $\Delta S = 2$ nonleptonic hyperon decays may serve as probes of new physics [1–3], where the BFs could be enhanced to the level of $10^{-10}$–$10^{-7}$ when beyond the SM effects are considered [1]. Though these BFs may still be beyond current experimental sensitivity, it is still worthwhile to search for these decays.

Until now, there have been many searches for the $\Delta S = 2$ decays in the spin 1/2 hyperon sector, such as $\mathcal{B}(\Xi^0 \to p\pi^-) < 8.2 \times 10^{-6}$ [4], $\mathcal{B}(\Xi^0 \to pe^-\bar{\nu}_e) < 1.3 \times 10^{-3}$ [5], $\mathcal{B}(\Xi^- \to n\pi^-) < 1.9 \times 10^{-5}$ [6], $\mathcal{B}(\Xi^- \to p\pi^-\pi^-) < 4.0 \times 10^{-4}$ [7], etc., which are all set at the 90% confidence level (C. L.). However, in the spin 3/2 hyperon sector, only one upper limit has been set, $\mathcal{B}(\Omega^- \to \Lambda\pi^-) < 2.9 \times 10^{-6}$ [4]. The potential $\Delta S = 2$ decays, $\Omega^- \to \Sigma^0\pi^-$ and $\Omega^- \to nK^-$, as illustrated in figure 1, have not been explored so far. According to ref. [1], the decay $\Omega^- \to nK^-$ could have different new physics contributions compared to the $\Omega^- \to \Lambda\pi^-$ decay. Therefore, it is of interest also to experimentally search for the decay $\Omega^- \to nK^-$, as well as $\Omega^- \to \Sigma^0\pi^-$.

In this paper, based on approximately $1.7 \times 10^5$ $\Omega^-\bar{\Omega}^+$ pairs [8] produced from $(27.12 \pm 0.14) \times 10^8$ $\psi(3686)$ events [9] collected with the BESIII detector in 2009, 2012 and 2021, we present the first searches for $\Omega^- \to \Sigma^0\pi^-$ and $\Omega^- \to nK^-$ decays (the charge conjugated decays are always implied), using a double-tag (DT) method. The single-tag (ST) $\bar{\Omega}^+$ hyperons are reconstructed via the decay $\bar{\Omega}^+ \to \bar{\Lambda}K^+$. Events where a signal candidate is reconstructed with the particles recoiling against the ST $\bar{\Omega}^+$ hyperon are DT events. The BF of a signal decay is determined by

$$\mathcal{B}_{\rm sig} = \frac{N_{\rm DT} \cdot \epsilon_{\rm ST}}{N_{\rm ST} \cdot \epsilon_{\rm DT}} = \frac{N_{\rm DT}}{N_{\rm ST} \cdot \epsilon_{\rm sig}}, \tag{1.1}$$

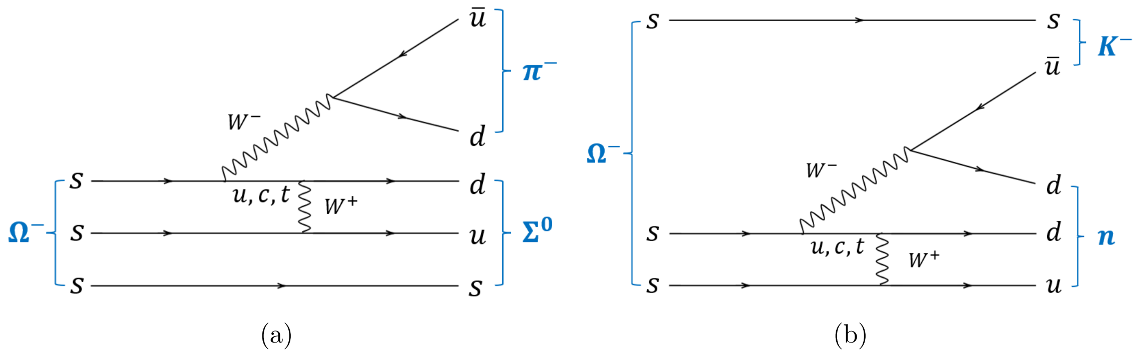


**Figure 1.** Feynman diagrams contributing to the $\Delta S = 2$ nonleptonic hyperon decays (a) $\Omega^- \to \Sigma^0\pi^-$ and (b) $\Omega^- \to nK^-$ in the SM.

where $N_{\rm ST}$ and $N_{\rm DT}$ represent the ST and DT yields, respectively, and $\epsilon_{\rm sig} = \epsilon_{\rm DT}/\epsilon_{\rm ST}$ is the signal efficiency in the presence of an ST $\bar{\Omega}^+$ hyperon, where $\epsilon_{\rm ST}$ and $\epsilon_{\rm DT}$ are the ST and DT efficiencies, respectively.

## 2 BESIII detector and Monte Carlo simulation

The BESIII detector [10, 11] records symmetric $e^+e^-$ collisions provided by the BEPCII storage ring [12, 13] in the center-of-mass energy range from 2.0 to 4.95 GeV, with a peak luminosity of $1.1 \times 10^{33}\,\text{cm}^{-2}\,\text{s}^{-1}$ achieved at $\sqrt{s} = 3.773$ GeV. The cylindrical core of the BESIII detector covers 93% of the full solid angle and consists of a helium-based multilayer drift chamber (MDC), a plastic scintillator time-of-flight system (TOF), and a CsI(Tl) electromagnetic calorimeter (EMC), which are all enclosed in a superconducting solenoidal magnet providing a 1.0 T (0.9 T in 2012) magnetic field. The solenoid is supported by an octagonal flux-return yoke with resistive plate counter muon identification modules interleaved with steel. The charged-particle momentum resolution at 1 GeV/$c$ is 0.5%, and the $dE/dx$ resolution is 6% for electrons from Bhabha scattering. The EMC measures photon energies with a resolution of 2.5% (5%) at 1 GeV in the barrel (end cap) region. The time resolution in the TOF barrel region is 68 ps, while that in the end cap region was 110 ps. The end cap TOF system was upgraded in 2015 using multigap resistive plate chamber technology, providing a time resolution of 60 ps, which benefits about 83% of the data used in this analysis [14–16].

Simulated data samples produced with the GEANT4-based [17] Monte Carlo (MC) software [18] which includes the geometric description of the BESIII detector and the detector response, are used to determine the detection efficiency and estimate the backgrounds. The simulation includes the beam energy spread and initial state radiation (ISR) in the $e^+e^-$ annihilations modeled with the generator KKMC [19]. A sample of simulated inclusive $\psi(3686)$ events, which includes both the production of the $\psi(3686)$ resonance and the continuum processes incorporated in KKMC, is used to estimate the background events.

All particle decays are modeled with EVTGEN [20, 21] using the BFs either taken from the PDG [7], when available, or otherwise estimated with LUNDCHARM [22, 23]. Final state radiation from charged final state particles is incorporated using PHOTOS [24]. For the signal decays, three signal MC samples are used. On the tag side, $\psi(3686) \to \Omega^-\bar{\Omega}^+$, $\bar{\Omega}^+ \to \bar{\Lambda}(\to$

$\bar{p}\pi^+)K^+$, which is generated according to the angular distributions measured in ref. [25], is used to determine the ST efficiency. The signal decays, $\Omega^- \to X$, $\Omega^- \to \Sigma^0(\to X)\pi^-$, and $\Omega^- \to nK^-$, are generated uniformly in phase space. The final state $X$ indicates inclusive decay. The first one is used to determine the ST efficiency, and the later two are used to determine the DT efficiencies. The ST sample consists of 2.54 million events. Each of the two DT samples contains 1.27 million events.

## 3 Data analysis

The decay chains of interest are $\psi(3686) \to \Omega^-\bar{\Omega}^+$, $\bar{\Omega}^+ \to \bar{\Lambda}(\to \bar{p}\pi^+)K^+$, $\Omega^- \to \Sigma^0(\to X)\pi^-$ and $\psi(3686) \to \Omega^-\bar{\Omega}^+$, $\bar{\Omega}^+ \to \bar{\Lambda}(\to \bar{p}\pi^+)K^+$, $\Omega^- \to nK^-$. The ST $\bar{\Omega}^+$ hyperons are reconstructed via the decay $\bar{\Omega}^+ \to \bar{\Lambda}K^+$. The charged tracks in the MDC are required to have a polar angle $\theta$ within the MDC acceptance $|\cos\theta| < 0.93$, where $\theta$ is defined with respect to the $z$-axis (the symmetry axis of the MDC). In order to perform particle identification (PID), the specific ionization energy loss $dE/dx$ and the time-of-flight information are combined to form a likelihood $\mathcal{L}(h)$ ($h = p, K, \pi$) for each hadron $h$ hypothesis. Charged tracks with $\mathcal{L}(p) > \mathcal{L}(K)$, $\mathcal{L}(p) > \mathcal{L}(\pi)$ and $\mathcal{L}(p) > 0.001$ are identified as protons, and those with $\mathcal{L}(K) > \mathcal{L}(\pi)$ and $\mathcal{L}(K) > 0$ as kaons. The remaining charged tracks are assigned as pions by default.

The $\bar{\Lambda}$ candidates are reconstructed from $\bar{p}\pi^+$ pairs, which are constrained to originate from a common vertex and are required to have an invariant mass within the range of $[1.111, 1.121]\,\mathrm{GeV}/c^2$. Vertex fits are performed to the $\bar{\Lambda}K^+$ pairs to improve the mass resolution of the $\bar{\Omega}^+$ candidates. If there are multiple $\bar{\Omega}^+$ candidates, the one with the smallest value of $|\Delta E| = |E_{\bar{\Omega}^+} - E_{\mathrm{beam}}|$ is selected for further analysis. Here, $E_{\bar{\Omega}^+}$ is the energy of the reconstructed $\bar{\Omega}^+$ candidate in the $e^+e^-$ center-of-mass system and $E_{\mathrm{beam}}$ is the beam energy. Additionally, the invariant mass of the $\bar{\Lambda}K^+$ combination ($M_{\bar{\Lambda}K^+}$) must be in the $\bar{\Omega}^+$ signal region, defined as $[1.664, 1.680]\,\mathrm{GeV}/c^2$.

To determine the ST yield, a fit is applied to the recoil-mass spectrum against the reconstructed $\bar{\Omega}^+$ ($RM_{\bar{\Omega}^+}$), as shown in figure 2. In the fit, the signal shape is described by the MC simulated shape convolved with a Gaussian function with free parameters, where the Gaussian function is used to account for the difference in mass resolution between data and MC simulation. The background shape is described by a second-order Chebychev polynomial. For the search for $\Omega^- \to \Sigma^0\pi^-$ and $\Omega^- \to nK^-$, the signal region of $RM_{\bar{\Omega}^+}$ is defined as $[1.652, 1.695]\,\mathrm{GeV}/c^2$. The number of ST $\bar{\Omega}^+$ hyperons in the signal region is determined to be $25819 \pm 188$, and the ST efficiency is estimated to be 21.11% based on MC simulation. Events in $\bar{\Omega}^+$ sideband region, defined as $M_{\bar{\Lambda}K^+} \in [1.648, 1.656] \cup [1.688, 1.696]\,\mathrm{GeV}/c^2$, are used to study the backgrounds in the $RM_{\bar{\Omega}^+}$ signal region, and we find that the background distribution is smooth with no peaking background.

Candidates for $\Omega^- \to \Sigma^0\pi^-$ are selected from the surviving tracks in the system recoiling against the ST $\bar{\Omega}^+$ hyperons. To improve the DT efficiency, only the bachelor $\pi^-$ (from $\Omega^-$ decay) is reconstructed in the signal side. The polar angle of the bachelor $\pi^-$ must satisfy $|\cos\theta| < 0.93$. The $\pi^-$ candidates are identified using information measured by the MDC ($dE/dx$), TOF, and EMC. The probabilities for the pion and kaon hypotheses are calculated,

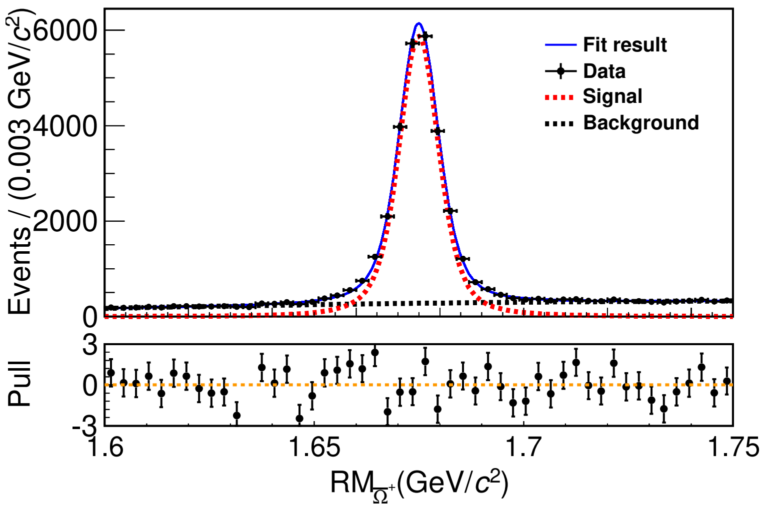


**Figure 2.** The distribution of $RM_{\bar{\Omega}^+}$. In the top panel, the dots with error bars are data, the blue solid line is the total fit result, and the black dashed and red dashed lines represent the fitted background and signal shapes, respectively. The bottom panel displays the pull distribution, illustrating the residuals between the data and the fitted model and normalized by their uncertainties.

and the pion candidate is required to satisfy $\mathcal{L}(\pi) > \mathcal{L}(K)$ and $\mathcal{L}(\pi) > 0$. If there is more than one $\pi^-$ candidate, the one with the highest momentum is retained.

For the decay $\Omega^- \to nK^-$, a similar approach is used, where only the bachelor $K^-$ (from $\Omega^-$ decay) is reconstructed on the signal side. The polar angle of the bachelor $K^-$ must satisfy $|\cos\theta| < 0.93$. The $K^-$ candidates are identified using the information measured by the MDC ($dE/dx$), TOF, and EMC. The probabilities for the kaon and pion hypotheses are calculated, and the kaon candidate is required to satisfy $\mathcal{L}(K) > \mathcal{L}(\pi)$ and $\mathcal{L}(K) > 0$. Additionally, the number of charged tracks ($N_{\rm tracks}$) including the single and tag sides is required to be four to further suppress background events.

The recoiling mass distribution of $\bar{\Omega}^+h$ ($RM_{\bar{\Omega}^+h}$) is used to extract the DT yield, where $h = \pi$ or $K$. Before that, potential backgrounds in the studies of $\Omega^- \to \Sigma^0\pi^-$ and $\Omega^- \to nK^-$ are investigated by analyzing the inclusive MC sample and the events in the $M_{\bar{\Lambda}K^+}$ and $RM_{\bar{\Omega}^+}$ sideband regions from data. The sideband regions in $RM_{\bar{\Omega}^+}$ are defined as $[1.718, 1.739] \cup [1.608, 1.630]$ GeV/$c^2$. For each decay, the background shape is found to be smooth in the $RM_{\bar{\Omega}^+h}$ spectrum. Then the number of DT events in data is obtained by fitting the $\bar{\Omega}^+h$ distribution. In the fit, the signal shape is described by the simulated shape derived from signal MC sample, and the background shape is described with a second-order Chebychev polynomial. The fit result is shown in figure 3. The numbers of DT events are $-15.4^{+10.0}_{-9.1}$ for $\Omega^- \to \Sigma^0\pi^-$ and $-8.3^{+5.5}_{-3.7}$ for $\Omega^- \to nK^-$. Since no significant signal is observed for each decay, we set upper limits on the BFs of these two decays.

## 4 Systematic uncertainty

The sources of systematic uncertainties are classified into two categories, which are multiplicative and additive. The multiplicative systematics affect the efficiency while the additive ones affect the signal yield.

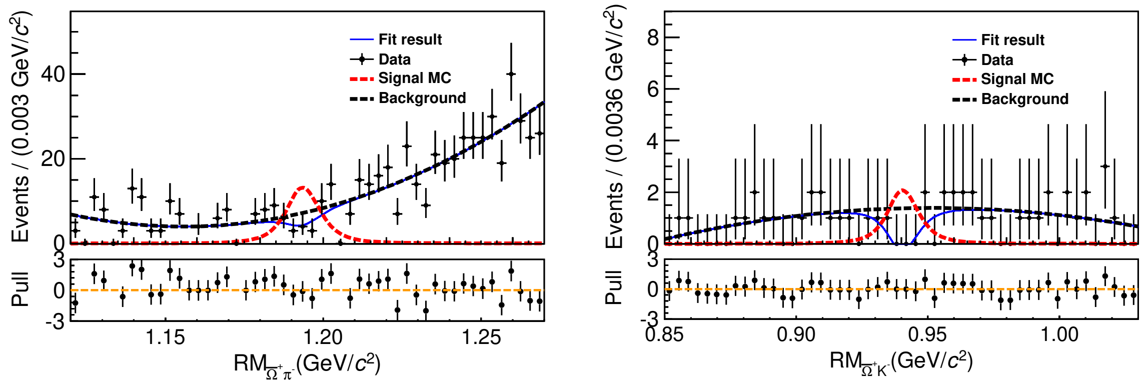


(a) (b)

**Figure 3.** The distributions of (a) $RM_{\bar{\Omega}^+\pi^-}$ and (b) $RM_{\bar{\Omega}^+K^-}$. In the top panel, the dots with error bars are data, the blue solid and black dashed lines are the total fit result and the fitted background shape, respectively. The red dashed line is the signal shape obtained from the signal MC with arbitrary normalization. The bottom panels display the pull distributions, illustrating the residuals between the data and the fitted model normalized by their uncertainties.

The multiplicative systematic uncertainties mainly stem from the imperfect modeling of data in our simulation. Considering the differences between MC simulation and data, the following sources are taken into account. The tracking and PID efficiencies of charged pions and kaons are investigated using the control samples of $J/\psi \to p\bar{p}\pi^+\pi^-$ and $J/\psi \to K^0_S K^\pm \pi^\mp$ [26–28], respectively. The differences in tracking and PID efficiencies between data and MC simulation are both 1.0% per charged pion on the signal side, and the uncertainties of the tracking and PID are both 1.0% per kaon on the signal side. The systematic uncertainty due to the signal model is studied by the control samples of $\Omega^- \to \Xi^0\pi^-$ and $\Omega^- \to \Lambda K^-$ [29]. The differences between the efficiencies obtained from phase space MC samples and data driven samples (re-weighted according to $\pi^-/K^-$ transverse momentum distribution in data) are taken as the systematic uncertainties, which are 2.2% and 6.9% for $\Omega^- \to \Sigma^0\pi^-$ and $\Omega^- \to nK^-$, respectively. The uncertainty from the $RM_{\bar{\Omega}^+}$ signal shape for ST is estimated by an alternative signal shape obtained from a Breit-Wigner convolved with a double Gaussian function with all free parameters. The resultant difference in the ST yield, 2.0%, is taken as the systematic uncertainty. Furthermore, the uncertainty due to the $RM_{\bar{\Omega}^+}$ background shape for ST is studied by changing the second-order Chebychev polynomial to a first-order and a third-order Chebychev polynomial. The larger difference in the ST yield, 0.7%, is considered as the corresponding uncertainty. The uncertainty due to the MC statistics is assigned by using the formula $\frac{1}{\sqrt{N}}\sqrt{\frac{1-\epsilon}{\epsilon}}$, where $\epsilon$ is the DT efficiency and $N$ is the number of the generated signal MC events. The systematic uncertainties are both 0.2% for $\Omega^- \to \Sigma^0\pi^-$ and $\Omega^- \to nK^-$. The statistical fluctuation of the ST $\bar{\Omega}^+$ hyperons, 0.7%, is taken as a systematic uncertainty from the ST yield estimation. The systematic uncertainty due to the signal angular distribution is studied by the control samples of $\Omega^- \to \Xi^0\pi^-$ and $\Omega^- \to \Lambda K^-$ [29]. In the search for $\Omega^- \to nK^-$, the systematic uncertainty of the requirement on the number of charged tracks is studied by using a control sample of $\psi(3686) \to \Omega^-\bar{\Omega}^+$, $\bar{\Omega}^+ \to \bar{\Lambda}(\to \bar{p}\pi^+)K^+$, $\Omega^- \to \Lambda(\to p\pi^-)K^-$. This control sample, comprising six charged



JHEP05(2024)141

| Source | $\Omega^- \to \Sigma^0\pi^-$ | $\Omega^- \to nK^-$ |
|---|---|---|
| Tracking | 1.0 | 1.0 |
| PID | 1.0 | 1.0 |
| ST signal shape | 2.0 | 2.0 |
| ST background shape | 0.7 | 0.7 |
| MC statistics | 0.2 | 0.2 |
| ST yields | 0.7 | 0.7 |
| Signal model | 2.2 | 6.9 |
| Number of charged tracks | — | 3.1 |
| Total | 3.4 | 8.0 |

**Table 1.** Multiplicative systematic uncertainties (%), where the dash (—) indicates that a systematic effect is not applicable.

tracks, is used to evaluate the efficiencies of the $N_{\text{tracks}} = 6$ requirement for data and MC. The efficiency difference between data and MC in the control sample, 3.1%, is taken as the systematic uncertainty. All the multiplicative uncertainties are summarized in table 1. The individual uncertainties are assumed to be independent and are combined in quadrature to obtain the total multiplicative systematic uncertainty. Note that the systematic uncertainty of the measurement of $\Omega^- \to nK^-$ is dominated by the signal model because the kaon reconstruction efficiency is heavily dependent on its transverse momentum.

There are two sources in the additive systematic uncertainties. One systematic uncertainty due to the $RM_{\bar{\Omega}^+h}$ signal shape is studied by changing the MC simulated shape to double Johnson functions [30] sharing the same mean and width parameters determined from the fit. The tail parameters and fractions of each signal component are fixed to values obtained from a fit to simulated events. Another systematic uncertainty due to the $RM_{\bar{\Omega}^+h}$ background shape is studied by changing the Chebychev polynomial from second to third order. The results are used to estimate the upper limits, described in the next section.

## 5 The upper limits on the BFs

The upper limits on the signal yields at the 90% C. L. are determined by a Bayesian method [31]. The additive uncertainties are accounted for by extracting the likelihood distributions, and the signal shapes corresponding to the maximum upper limits among all additive items are chosen for $\Omega^- \to \Sigma^0\pi^-$ and $\Omega^- \to nK^-$, respectively. The upper limits based on these likelihood distributions and incorporating the multiplicative systematic uncertainties in the calculation are obtained by smearing the likelihood distribution by a Gaussian function with a mean of zero and a width equal to $\sigma_\epsilon$ as described in refs. [32, 33] with the following formula,

$$L'(n) \propto \int_0^1 L\left(n\frac{\epsilon}{\epsilon_0}\right) \exp\left[\frac{-(\epsilon-\epsilon_0)^2}{2\sigma_\epsilon^2}\right] d\epsilon, \tag{5.1}$$

where $L(n)$ is the likelihood distribution as a function of the yield $n$. $\epsilon_0$ is the signal efficiency and $\sigma_\epsilon$ is the multiplicative systematic uncertainty. The signal yield at the 90% C.L., $N^{\text{U.L.}}$,



JHEP05(2024)141

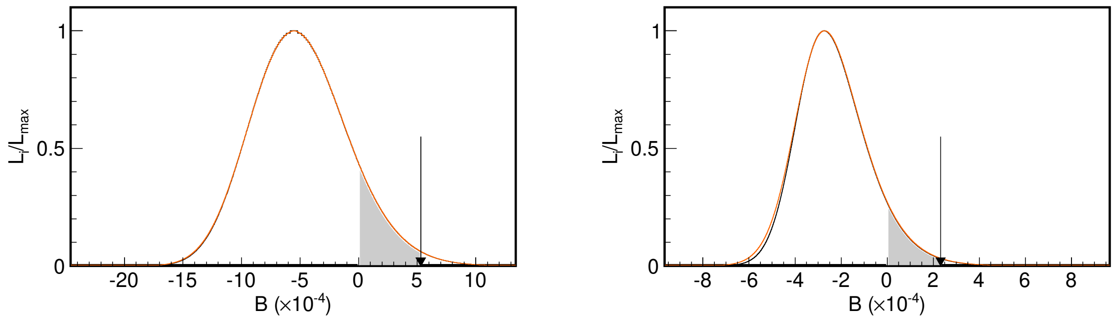


(a) (b)

**Figure 4.** The normalized likelihood distributions for (a) $\Omega^- \to \Sigma^0\pi^-$ and (b) $\Omega^- \to nK^-$. The orange curves are obtained with incorporating both multiplicative and additive systematic uncertainties. The black curves are the likelihood distributions without multiplicative systematic uncertainties. The arrows point the upper limit on the BFs at the 90% C.L.

| Decay mode | $N_{\rm ST}$ | $\epsilon_{\rm ST}$ (%) | $N_{\rm DT}^{\rm U.L.}$ | $\epsilon_{\rm DT}$ (%) | $\mathcal{B}^{\rm U.L.}$ ($\times 10^{-4}$) |
|---|---|---|---|---|---|
| $\Omega^- \to \Sigma^0\pi^-$ | $25819 \pm 188$ | 21.11 | 12 | 18.29 | 5.4 |
| $\Omega^- \to nK^-$ | | | 5 | 16.92 | 2.4 |

**Table 2.** The ST yield ($N_{\rm ST}$), ST efficiency ($\epsilon_{\rm ST}$), DT yields ($N_{\rm DT}^{\rm U.L.}$), DT efficiencies ($\epsilon_{\rm DT}$) and the upper limits on the BFs ($\mathcal{B}^{\rm U.L.}$).

is obtained by integrating out to 90% of its physical region, $\frac{\int_0^{N^{\rm U.L.}} L'(n)dn}{\int_0^{\infty} L'(n)dn} = 0.9$. Figures 4(a) and 4(b) show the likelihood distributions incorporating the systematic uncertainties for $\Omega^- \to \Sigma^0\pi^-$ and $\Omega^- \to nK^-$, respectively. The upper limits on the signal yields ($N_{\rm DT}^{\rm U.L.}$) of $\Omega^- \to \Sigma^0\pi^-$ and $\Omega^- \to nK^-$ at the 90% C.L. are 12 and 5, respectively. With the ST yields, and the ST and DT efficiencies obtained from the MC simulation, the upper limits on the BFs on the signal decays at the 90% C.L. are calculated by

$$\mathcal{B}_{\rm sig}^{\rm U.L.} = \frac{N_{\rm DT}^{\rm U.L.}/\epsilon_{\rm DT}}{N_{\rm ST}/\epsilon_{\rm ST}}. \tag{5.2}$$

The numerical results are shown in table 2.

## 6 Summary

Based on the sample of $(27.12 \pm 0.14) \times 10^8$ $\psi(3686)$ events collected by the BESIII detector, we search for the $\Delta S = 2$ decays of $\Omega^- \to \Sigma^0\pi^-$ and $\Omega^- \to nK^-$ for the first time. No signal is observed. The upper limits on their decay BFs are determined to be $\mathcal{B}(\Omega^- \to \Sigma^0\pi^-) < 5.4 \times 10^{-4}$ and $\mathcal{B}(\Omega^- \to nK^-) < 2.4 \times 10^{-4}$ at the 90% C.L. These results are consistent with the predictions of the SM [1] and can help to constrain new physics models. In the future, the proposed Super Tau-Charm Factories [34, 35] have the potential to improve on the upper limits on the BFs of these decays by at least two orders of magnitude.

JHEP05(2024)141

## Acknowledgments

The BESIII collaboration thanks the staff of BEPCII and the IHEP computing center for their strong support. The authors would like to extend thanks to Prof. Jusak Tandean for useful discussion and helpful advice. This work is supported in part by National Key R&D Program of China under Contracts Nos. 2020YFA0406300, 2020YFA0406400; National Natural Science Foundation of China (NSFC) under Contracts Nos. 11635010, 11735014, 11835012, 11935015, 11935016, 11935018, 11961141012, 12025502, 12035009, 12035013, 12061131003, 12192260, 12192261, 12192262, 12192263, 12192264, 12192265, 12221005, 12225509, 12235017, 12342502; the Chinese Academy of Sciences (CAS) Large-Scale Scientific Facility Program; the CAS Center for Excellence in Particle Physics (CCEPP); Joint Large-Scale Scientific Facility Funds of the NSFC and CAS under Contract No. U1832207; CAS Key Research Program of Frontier Sciences under Contracts Nos. QYZDJ-SSW-SLH003, QYZDJ-SSW-SLH040; 100 Talents Program of CAS; The Institute of Nuclear and Particle Physics (INPAC) and Shanghai Key Laboratory for Particle Physics and Cosmology; European Union's Horizon 2020 research and innovation programme under Marie Sklodowska-Curie grant agreement under Contract No. 894790; German Research Foundation DFG under Contracts Nos. 455635585, Collaborative Research Center CRC 1044, FOR5327, GRK 2149; Istituto Nazionale di Fisica Nucleare, Italy; Ministry of Development of Turkey under Contract No. DPT2006K-120470; National Research Foundation of Korea under Contract No. NRF-2022R1A2C1092335; National Science and Technology fund of Mongolia; National Science Research and Innovation Fund (NSRF) via the Program Management Unit for Human Resources & Institutional Development, Research and Innovation of Thailand under Contract No. B16F640076; Polish National Science Centre under Contract No. 2019/35/O/ST2/02907; The Swedish Research Council; U.S. Department of Energy under Contract No. DE-FG02-05ER41374.



## References

[1] X.-G. He, J. Tandean and G. Valencia, $\Delta S = 2$ *nonleptonic hyperon decays as probes of new physics*, *Phys. Rev. D* **108** (2023) 055012 [arXiv:2304.02559] [INSPIRE].

[2] X.-G. He and G. Valencia, $\Delta I = 3/2$ *and* $\Delta S = 2$ *hyperon decays in chiral perturbation theory*, *Phys. Lett. B* **409** (1997) 469 [*Erratum ibid.* **418** (1998) 443] [hep-ph/9705462] [INSPIRE].

[3] S.L. Glashow, *Direct* $\Xi$ *Decay and Muonium-Antimuonium Transitions*, *Phys. Rev. Lett.* **6** (1961) 196 [INSPIRE].

[4] HyperCP collaboration, *Search for* $\Delta S = 2$ *nonleptonic hyperon decays*, *Phys. Rev. Lett.* **94** (2005) 101804 [hep-ex/0503036] [INSPIRE].

[5] P.M. Dauber, J.P. Berge, J.R. Hubbard, D.W. Merrill and R.A. Muller, *Production and decay of cascade hyperons*, *Phys. Rev.* **179** (1969) 1262 [INSPIRE].

[6] S.F. Biagi et al., *A new upper limit for the branching ratio* $\Xi^- \to n\pi^-/\Xi^- \to \Lambda\pi^-$, *Phys. Lett. B* **112** (1982) 277 [INSPIRE].

[7] Particle Data collaboration, *Review of Particle Physics*, *Prog. Theor. Exp. Phys.* **2022** (2022) 083C01 [inSPIRE].

[8] H.-B. Li, *Prospects for rare and forbidden hyperon decays at BESIII*, *Front. Phys.* **12** (2017) 121301 [*Erratum ibid.* **14** (2019) 64001] [arXiv:1612.01775] [inSPIRE].

[9] BESIII collaboration, *Determination of the number of $\psi(3686)$ events taken at BESIII*, arXiv:2403.06766 [inSPIRE].

[10] BESIII collaboration, *Design and Construction of the BESIII Detector*, *Nucl. Instrum. Meth. A* **614** (2010) 345 [arXiv:0911.4960] [inSPIRE].

[11] BESIII collaboration, *Future Physics Programme of BESIII*, *Chin. Phys. C* **44** (2020) 040001 [arXiv:1912.05983] [inSPIRE].

[12] C. Yu et al., *BEPCII Performance and Beam Dynamics Studies on Luminosity*, in the proceedings of the *7th International Particle Accelerator Conference*, Busan, South Korea, 8–13 May 2016 [DOI:10.18429/JACoW-IPAC2016-TUYA01] [inSPIRE].

[13] K.-X. Huang et al., *Method for detector description transformation to Unity and application in BESIII*, *Nucl. Sci. Tech.* **33** (2022) 142 [arXiv:2206.10117] [inSPIRE].

[14] X. Li et al., *Study of MRPC technology for BESIII endcap-TOF upgrade*, *Radiat. Detect. Technol. Meth.* **1** (2017) 13 [inSPIRE].

[15] Y.-X. Guo et al., *The study of time calibration for upgraded end cap TOF of BESIII*, *Radiat. Detect. Technol. Meth.* **1** (2017) 15 [inSPIRE].

[16] P. Cao et al., *Design and construction of the new BESIII endcap Time-of-Flight system with MRPC Technology*, *Nucl. Instrum. Meth. A* **953** (2020) 163053 [inSPIRE].

[17] GEANT4 collaboration, *GEANT4 — a simulation toolkit*, *Nucl. Instrum. Meth. A* **506** (2003) 250 [inSPIRE].

[18] Z. Deng et al., *Object-oriented BESIII detector simulation system*, *High Energy Phys. Nucl. Phys.* **30** (2006) 371.

[19] S. Jadach, B.F.L. Ward and Z. Was, *Coherent exclusive exponentiation for precision Monte Carlo calculations*, *Phys. Rev. D* **63** (2001) 113009 [hep-ph/0006359] [inSPIRE].

[20] D.J. Lange, *The EvtGen particle decay simulation package*, *Nucl. Instrum. Meth. A* **462** (2001) 152 [inSPIRE].

[21] R.-G. Ping, *Event generators at BESIII*, *Chin. Phys. C* **32** (2008) 599 [inSPIRE].

[22] J.C. Chen, G.S. Huang, X.R. Qi, D.H. Zhang and Y.S. Zhu, *Event generator for $J/\psi$ and $\psi(2s)$ decay*, *Phys. Rev. D* **62** (2000) 034003 [inSPIRE].

[23] R.-L. Yang, R.-G. Ping and H. Chen, *Tuning and Validation of the Lundcharm Model with $J/\psi$ Decays*, *Chin. Phys. Lett.* **31** (2014) 061301 [inSPIRE].

[24] BESIII collaboration, *Branching fraction measurements of $\chi_{c0}$ and $\chi_{c2}$ to $\pi^0\pi^0$ and $\eta\eta$*, *Phys. Rev. D* **81** (2010) 052005 [arXiv:1001.5360] [inSPIRE].

[25] BESIII collaboration, *Model-Independent Determination of the Spin of the $\Omega^-$ and Its Polarization Alignment in $\psi(3686) \to \Omega^-\bar{\Omega}^+$*, *Phys. Rev. Lett.* **126** (2021) 092002 [arXiv:2007.03679] [inSPIRE].

[26] BESIII collaboration, *Search for a light Higgs-like boson $A^0$ in $J/\psi$ radiative decays*, *Phys. Rev. D* **85** (2012) 092012 [arXiv:1111.2112] [inSPIRE].

[27] BESIII collaboration, *Study of $\chi_{cJ}$ radiative decays into a vector meson*, *Phys. Rev. D* **83** (2011) 112005 [arXiv:1103.5564] [INSPIRE].

[28] BESIII collaboration, *Tests of CP symmetry in entangled $\Xi^0$–$\bar{\Xi}^0$ pairs*, *Phys. Rev. D* **108** (2023) L031106 [arXiv:2305.09218] [INSPIRE].

[29] BESIII collaboration, *Measurements of the absolute branching fractions of $\Omega$-decays and test of the $\Delta I = 1/2$ rule*, *Phys. Rev. D* **108** (2023) L091101 [arXiv:2309.06368] [INSPIRE].

[30] N.L. Johnson, *Systems of frequency curves generated by methods of translation*, *Biometrika* **36** (1949) 149 [INSPIRE].

[31] G.J. Feldman and R.D. Cousins, *A Unified approach to the classical statistical analysis of small signals*, *Phys. Rev. D* **57** (1998) 3873 [physics/9711021] [INSPIRE].

[32] K. Stenson, *A more exact solution for incorporating multiplicative systematic uncertainties in branching ratio limits*, physics/0605236 [INSPIRE].

[33] X.-X. Liu, X.-R. Lü and Y.S. Zhu, *Combined estimation for multi-measurements of branching ratio*, *Chin. Phys. C* **39** (2015) 103001 [arXiv:1505.01278] [INSPIRE].

[34] Charm-Tau Factory collaboration, *Project of a Super Charm-Tau factory at the Budker Institute of Nuclear Physics in Novosibirsk*, *Phys. Atom. Nucl.* **76** (2013) 1072 [INSPIRE].

[35] M. Achasov et al., *STCF conceptual design report (Volume 1): Physics & detector*, *Front. Phys.* **19** (2024) 14701 [arXiv:2303.15790] [INSPIRE].


JHEP05(2024)141

## The BESIII collaboration

M. Ablikim[1], M.N. Achasov[4,c], P. Adlarson[75], O. Afedulidis[3], X.C. Ai[80], R. Aliberti[35], A. Amoroso[74A,74C], Q. An[71,58,a], Y. Bai[57], O. Bakina[36], I. Balossino[29A], Y. Ban[46,h], H.-R. Bao[63], V. Batozskaya[1,44], K. Begzsuren[32], N. Berger[35], M. Berlowski[44], M. Bertani[28A], D. Bettoni[29A], F. Bianchi[74A,74C], E. Bianco[74A,74C], A. Bortone[74A,74C], I. Boyko[36], R.A. Briere[5], A. Brueggemann[68], H. Cai[76], X. Cai[1,58], A. Calcaterra[28A], G.F. Cao[1,63], N. Cao[1,63], S.A. Cetin[62A], J.F. Chang[1,58], G.R. Che[43], G. Chelkov[36,b], C. Chen[43], C.H. Chen[9], Chao Chen[55], G. Chen[1], H.S. Chen[1,63], H.Y. Chen[20], M.L. Chen[1,58,63], S.J. Chen[42], S.L. Chen[45], S.M. Chen[61], T. Chen[1,63], X.R. Chen[31,63], X.T. Chen[1,63], Y.B. Chen[1,58], Y.Q. Chen[34], Z.J. Chen[25,i], Z.Y. Chen[1,63], S.K. Choi[10], G. Cibinetto[29A], F. Cossio[74C], J.J. Cui[50], H.L. Dai[1,58], J.P. Dai[78], A. Dbeyssi[18], R.E. de Boer[3], D. Dedovich[36], C.Q. Deng[72], Z.Y. Deng[1], A. Denig[35], I. Denysenko[36], M. Destefanis[74A,74C], F. De Mori[74A,74C], B. Ding[66,1], X.X. Ding[46,h], Y. Ding[40], Y. Ding[34], J. Dong[1,58], L.Y. Dong[1,63], M.Y. Dong[1,58,63], X. Dong[76], M.C. Du[1], S.X. Du[80], Y.Y. Duan[55], Z.H. Duan[42], P. Egorov[36,b], Y.H. Fan[45], J. Fang[59], J. Fang[1,58], S.S. Fang[1,63], W.X. Fang[1], Y. Fang[1], Y.Q. Fang[1,58], R. Farinelli[29A], L. Fava[74B,74C], F. Feldbauer[3], G. Felici[28A], C.Q. Feng[71,58], J.H. Feng[59], Y.T. Feng[71,58], M. Fritsch[3], C.D. Fu[1], J.L. Fu[63], Y.W. Fu[1,63], H. Gao[63], X.B. Gao[41], Y.N. Gao[46,h], Yang Gao[71,58], S. Garbolino[74C], I. Garzia[29A,29B], L. Ge[80], P.T. Ge[76], Z.W. Ge[42], C. Geng[59], E.M. Gersabeck[67], A. Gilman[69], K. Goetzen[13], L. Gong[40], W.X. Gong[1,58], W. Gradl[35], S. Gramigna[29A,29B], M. Greco[74A,74C], M.H. Gu[1,58], Y.T. Gu[15], C.Y. Guan[1,63], A.Q. Guo[31,63], L.B. Guo[41], M.J. Guo[50], R.P. Guo[49], Y.P. Guo[12,g], A. Guskov[36,b], J. Gutierrez[27], K.L. Han[63], T.T. Han[1], F. Hanisch[3], X.Q. Hao[19], F.A. Harris[65], K.K. He[55], K.L. He[1,63], F.H. Heinsius[3], C.H. Heinz[35], Y.K. Heng[1,58,63], C. Herold[60], T. Holtmann[3], P.C. Hong[34], G.Y. Hou[1,63], X.T. Hou[1,63], Y.R. Hou[63], Z.L. Hou[1], B.Y. Hu[59], H.M. Hu[1,63], J.F. Hu[56,j], S.L. Hu[12,g], T. Hu[1,58,63], Y. Hu[1], G.S. Huang[71,58], K.X. Huang[59], L.Q. Huang[31,63], X.T. Huang[50], Y.P. Huang[1], Y.S. Huang[59], T. Hussain[73], F. Hölzken[3], N. Hüsken[35], N. in der Wiesche[68], J. Jackson[27], S. Janchiv[32], J.H. Jeong[10], Q. Ji[1], Q.P. Ji[19], W. Ji[1,63], X.B. Ji[1,63], X.L. Ji[1,58], Y.Y. Ji[50], X.Q. Jia[50], Z.K. Jia[71,58], D. Jiang[1,63], H.B. Jiang[76], P.C. Jiang[46,h], S.S. Jiang[39], T.J. Jiang[16], X.S. Jiang[1,58,63], Y. Jiang[63], J.B. Jiao[50], J.K. Jiao[34], Z. Jiao[23], S. Jin[42], Y. Jin[66], M.Q. Jing[1,63], X.M. Jing[63], T. Johansson[75], S. Kabana[33], N. Kalantar-Nayestanaki[64], X.L. Kang[9], X.S. Kang[40], M. Kavatsyuk[64], B.C. Ke[80], V. Khachatryan[27], A. Khoukaz[68], R. Kiuchi[1], O.B. Kolcu[62A], B. Kopf[3], M. Kuessner[3], X. Kui[1,63], N. Kumar[26], A. Kupsc[44,75], W. Kühn[37], J.J. Lane[67], P. Larin[18], L. Lavezzi[74A,74C], T.T. Lei[71,58], Z.H. Lei[71,58], M. Lellmann[35], T. Lenz[35], C. Li[43], C. Li[47], C.H. Li[39], Cheng Li[71,58], D.M. Li[80], F. Li[1,58], G. Li[1], H.B. Li[1,63], H.J. Li[19], H.N. Li[56,j], Hui Li[43], J.R. Li[61], J.S. Li[59], K. Li[1], L.J. Li[1,63], L.K. Li[1], Lei Li[48], M.H. Li[43], P.R. Li[38,k,l], Q.M. Li[1,63], Q.X. Li[50], R. Li[17,31], S.X. Li[12], T. Li[50], W.D. Li[1,63], W.G. Li[1,a], X. Li[1,63], X.H. Li[71,58], X.L. Li[50], X.Y. Li[1,63], X.Z. Li[59], Y.G. Li[46,h], Z.J. Li[59], Z.Y. Li[78], C. Liang[42], H. Liang[1,63], H. Liang[71,58], Y.F. Liang[54], Y.T. Liang[31,63], G.R. Liao[14], L.Z. Liao[50], Y.P. Liao[1,63], J. Libby[26], A. Limphirat[60], C.C. Lin[55], D.X. Lin[31,63], T. Lin[1], B.J. Liu[1], B.X. Liu[76], C. Liu[34], C.X. Liu[1], F. Liu[1], F.H. Liu[53], Feng Liu[6], G.M. Liu[56,j], H. Liu[38,k,l], H.B. Liu[15], H.H. Liu[1], H.M. Liu[1,63], Huihui Liu[21], J.B. Liu[71,58], J.Y. Liu[1,63], K. Liu[38,k,l], K.Y. Liu[40], Ke Liu[22], L. Liu[71,58], L.C. Liu[43], Lu Liu[43], M.H. Liu[12,g], P.L. Liu[1], Q. Liu[63], S.B. Liu[71,58], T. Liu[12,g], W.K. Liu[43], W.M. Liu[71,58], X. Liu[38,k,l], X. Liu[39], Y. Liu[80], Y. Liu[38,k,l], Y.B. Liu[43], Z.A. Liu[1,58,63], Z.D. Liu[9], Z.Q. Liu[50], X.C. Lou[1,58,63], F.X. Lu[59], H.J. Lu[23], J.G. Lu[1,58], X.L. Lu[1], Y. Lu[7], Y.P. Lu[1,58], Z.H. Lu[1,63], C.L. Luo[41], J.R. Luo[59], M.X. Luo[79], T. Luo[12,g], X.L. Luo[1,58], X.R. Lyu[63], Y.F. Lyu[43], F.C. Ma[40], H. Ma[78], H.L. Ma[1], J.L. Ma[1,63], L.L. Ma[50], M.M. Ma[1,63], Q.M. Ma[1], R.Q. Ma[1,63], T. Ma[71,58], X.T. Ma[1,63], X.Y. Ma[1,58], Y. Ma[46,h], Y.M. Ma[31], F.E. Maas[18], M. Maggiora[74A,74C], S. Malde[69], Y.J. Mao[46,h], Z.P. Mao[1], S. Marcello[74A,74C], Z.X. Meng[66], J.G. Messchendorp[13,64], G. Mezzadri[29A], H. Miao[1,63], T.J. Min[42], R.E. Mitchell[27], X.H. Mo[1,58,63], B. Moses[27], N.Yu. Muchnoi[4,c], J. Muskalla[35], Y. Nefedov[36], F. Nerling[18,e], L.S. Nie[20], I.B. Nikolaev[4,c], Z. Ning[1,58], S. Nisar[11,m], Q.L. Niu[38,k,l], W.D. Niu[55], Y. Niu[50], S.L. Olsen[63], Q. Ouyang[1,58,63], S. Pacetti[28B,28C], X. Pan[55], Y. Pan[57], A. Pathak[34], P. Patteri[28A], Y.P. Pei[71,58], M. Pelizaeus[3], H.P. Peng[71,58], Y.Y. Peng[38,k,l], K. Peters[13,e], J.L. Ping[41], R.G. Ping[1,63], S. Plura[35], V. Prasad[33], F.Z. Qi[1], H. Qi[71,58], H.R. Qi[61], M. Qi[42], T.Y. Qi[12,g], S. Qian[1,58], W.B. Qian[63], C.F. Qiao[63], X.K. Qiao[80], J.J. Qin[72], L.Q. Qin[14], L.Y. Qin[71,58], X.S. Qin[50], Z.H. Qin[1,58], J.F. Qiu[1], Z.H. Qu[72], C.F. Redmer[35], K.J. Ren[39], A. Rivetti[74C], M. Rolo[74C], G. Rong[1,63], Ch. Rosner[18], S.N. Ruan[43], N. Salone[44], A. Sarantsev[36,d], Y. Schelhaas[35], K. Schoenning[75], M. Scodeggio[29A], K.Y. Shan[12,g], W. Shan[24], X.Y. Shan[71,58], Z.J. Shang[38,k,l], J.F. Shangguan[16], L.G. Shao[1,63], M. Shao[71,58], C.P. Shen[12,g], H.F. Shen[1,8], W.H. Shen[63], X.Y. Shen[1,63], B.A. Shi[63], H. Shi[71,58], H.C. Shi[71,58], J.L. Shi[12,g], J.Y. Shi[1], Q.Q. Shi[55], S.Y. Shi[72], X. Shi[1,58], J.J. Song[19], T.Z. Song[59], W.M. Song[34,1], Y.J. Song[12,g], Y.X. Song[46,h,n], S. Sosio[74A,74C], S. Spataro[74A,74C], F. Stieler[35], Y.J. Su[63], G.B. Sun[76], G.X. Sun[1], H. Sun[63], H.K. Sun[1], J.F. Sun[19], K. Sun[61], L. Sun[76], S.S. Sun[1,63], T. Sun[51,f], W.Y. Sun[34], Y. Sun[9], Y.J. Sun[71,58], Y.Z. Sun[1], Z.Q. Sun[1,63], Z.T. Sun[50], C.J. Tang[54], G.Y. Tang[1], J. Tang[59], M. Tang[71,58], Y.A. Tang[76], L.Y. Tao[72], Q.T. Tao[25,i], M. Tat[69], J.X. Teng[71,58], V. Thoren[75], W.H. Tian[59], Y. Tian[31,63], Z.F. Tian[76], I. Uman[62B], Y. Wan[55], S.J. Wang[50], B. Wang[1], B.L. Wang[63], Bo Wang[71,58], D.Y. Wang[46,h], F. Wang[72], H.J. Wang[38,k,l], J.J. Wang[76], J.P. Wang[50], K. Wang[1,58], L.L. Wang[1], M. Wang[50], N.Y. Wang[63], S. Wang[12,g], S. Wang[38,k,l], T. Wang[12,g], T.J. Wang[43], W. Wang[72], W. Wang[59], W.P. Wang[35,71,o], X. Wang[46,h], X.F. Wang[38,k,l], X.J. Wang[39], X.L. Wang[12,g], X.N. Wang[1], Y. Wang[61], Y.D. Wang[45], Y.F. Wang[1,58,63], Y.L. Wang[19], Y.N. Wang[45], Y.Q. Wang[1], Yaqian Wang[17], Yi Wang[61], Z. Wang[1,58], Z.L. Wang[72], Z.Y. Wang[1,63], Ziyi Wang[63], D.H. Wei[14], F. Weidner[68], S.P. Wen[1], Y.R. Wen[39], U. Wiedner[3], G. Wilkinson[69], M. Wolke[75], L. Wollenberg[3], C. Wu[39], J.F. Wu[1,8], L.H. Wu[1], L.J. Wu[1,63], X. Wu[12,g], X.H. Wu[34], Y. Wu[71,58], Y.H. Wu[55], Y.J. Wu[31], Z. Wu[1,58], L. Xia[71,58], X.M. Xian[39], B.H. Xiang[1,63], T. Xiang[46,h], D. Xiao[38,k,l], G.Y. Xiao[42], S.Y. Xiao[1], Y.L. Xiao[12,g], Z.J. Xiao[41], C. Xie[42], X.H. Xie[46,h], Y. Xie[50], Y.G. Xie[1,58], Y.H. Xie[6], Z.P. Xie[71,58], T.Y. Xing[1,63], C.F. Xu[1,63], C.J. Xu[59], G.F. Xu[1], H.Y. Xu[66,2,p], M. Xu[71,58], Q.J. Xu[16], Q.N. Xu[30], W. Xu[1], W.L. Xu[66], X.P. Xu[55], Y.C. Xu[77], Z.P. Xu[42], Z.S. Xu[63], F. Yan[12,g], L. Yan[12,g], W.B. Yan[71,58], W.C. Yan[80], X.Q. Yan[1], H.J. Yang[51,f], H.L. Yang[34], H.X. Yang[1], T. Yang[1], Y. Yang[12,g], Y.F. Yang[43], Y.F. Yang[1,63], Y.X. Yang[1,63], Z.W. Yang[38,k,l], Z.P. Yao[50], M. Ye[1,58], M.H. Ye[8], J.H. Yin[1], Z.Y. You[59], B.X. Yu[1,58,63], C.X. Yu[43], G. Yu[1,63], J.S. Yu[25,i], T. Yu[72], X.D. Yu[46,h], Y.C. Yu[80], C.Z. Yuan[1,63], J. Yuan[45], J. Yuan[34], L. Yuan[2], S.C. Yuan[1,63], Y. Yuan[1,63], Z.Y. Yuan[59], C.X. Yue[39], A.A. Zafar[73], F.R. Zeng[50], S.H. Zeng[72], X. Zeng[12,g], Y. Zeng[25,i], Y.J. Zeng[1,63], Y.J. Zeng[59], X.Y. Zhai[34], Y.C. Zhai[50], Y.H. Zhan[59], A.Q. Zhang[1,63], B.L. Zhang[1,63], B.X. Zhang[1], D.H. Zhang[43], G.Y. Zhang[19], H. Zhang[80], H. Zhang[71,58], H.C. Zhang[1,58,63], H.H. Zhang[59], H.H. Zhang[34], H.Q. Zhang[1,58,63], H.R. Zhang[71,58], H.Y. Zhang[1,58], J. Zhang[80], J. Zhang[59], J.J. Zhang[52], J.L. Zhang[20], J.Q. Zhang[41], J.S. Zhang[12,g], J.W. Zhang[1,58,63], J.X. Zhang[38,k,l], J.Y. Zhang[1], J.Z. Zhang[1,63], Jianyu Zhang[63], L.M. Zhang[61], Lei Zhang[42], P. Zhang[1,63], Q.Y. Zhang[34], R.Y. Zhang[38,k,l], S.H. Zhang[1,63], Shulei Zhang[25,i], X.D. Zhang[45], X.M. Zhang[1], X.Y. Zhang[50], Y. Zhang[72], Y. Zhang[1], Y.T. Zhang[80], Y.H. Zhang[1,58], Y.M. Zhang[39], Yan Zhang[71,58], Z.D. Zhang[1], Z.H. Zhang[1], Z.L. Zhang[34], Z.Y. Zhang[43], Z.Y. Zhang[76], Z.Z. Zhang[45], G. Zhao[1], J.Y. Zhao[1,63], J.Z. Zhao[1,58], L. Zhao[1], Lei Zhao[71,58], M.G. Zhao[43], N. Zhao[78], R.P. Zhao[63], S.J. Zhao[80], Y.B. Zhao[1,58], Y.X. Zhao[31,63], Z.G. Zhao[71,58], A. Zhemchugov[36,b], B. Zheng[72], B.M. Zheng[34], J.P. Zheng[1,58], W.J. Zheng[1,63], Y.H. Zheng[63], B. Zhong[41], X. Zhong[59], H. Zhou[50], J.Y. Zhou[34], L.P. Zhou[1,63], S. Zhou[6], X. Zhou[76], X.K. Zhou[6], X.R. Zhou[71,58], X.Y. Zhou[39], Y.Z. Zhou[12,g], J. Zhu[43], K. Zhu[1], K.J. Zhu[1,58,63], K.S. Zhu[12,g], L. Zhu[34], L.X. Zhu[63], S.H. Zhu[70], S.Q. Zhu[42], T.J. Zhu[12,g], W.D. Zhu[41], Y.C. Zhu[71,58], Z.A. Zhu[1,63], J.H. Zou[1], J. Zu[71,58]

[1] *Institute of High Energy Physics, Beijing 100049, People's Republic of China*
[2] *Beihang University, Beijing 100191, People's Republic of China*
[3] *Bochum Ruhr-University, D-44780 Bochum, Germany*
[4] *Budker Institute of Nuclear Physics SB RAS (BINP), Novosibirsk 630090, Russia*
[5] *Carnegie Mellon University, Pittsburgh, Pennsylvania 15213, USA*
[6] *Central China Normal University, Wuhan 430079, People's Republic of China*
[7] *Central South University, Changsha 410083, People's Republic of China*
[8] *China Center of Advanced Science and Technology, Beijing 100190, People's Republic of China*
[9] *China University of Geosciences, Wuhan 430074, People's Republic of China*
[10] *Chung-Ang University, Seoul, 06974, Republic of Korea*
[11] *COMSATS University Islamabad, Lahore Campus, Defence Road, Off Raiwind Road, 54000 Lahore, Pakistan*
[12] *Fudan University, Shanghai 200433, People's Republic of China*
[13] *GSI Helmholtzcentre for Heavy Ion Research GmbH, D-64291 Darmstadt, Germany*
[14] *Guangxi Normal University, Guilin 541004, People's Republic of China*
[15] *Guangxi University, Nanning 530004, People's Republic of China*
[16] *Hangzhou Normal University, Hangzhou 310036, People's Republic of China*
[17] *Hebei University, Baoding 071002, People's Republic of China*
[18] *Helmholtz Institute Mainz, Staudinger Weg 18, D-55099 Mainz, Germany*
[19] *Henan Normal University, Xinxiang 453007, People's Republic of China*
[20] *Henan University, Kaifeng 475004, People's Republic of China*
[21] *Henan University of Science and Technology, Luoyang 471003, People's Republic of China*
[22] *Henan University of Technology, Zhengzhou 450001, People's Republic of China*
[23] *Huangshan College, Huangshan 245000, People's Republic of China*
[24] *Hunan Normal University, Changsha 410081, People's Republic of China*
[25] *Hunan University, Changsha 410082, People's Republic of China*
[26] *Indian Institute of Technology Madras, Chennai 600036, India*
[27] *Indiana University, Bloomington, Indiana 47405, USA*
[28] *INFN Laboratori Nazionali di Frascati , (A)INFN Laboratori Nazionali di Frascati, I-00044, Frascati, Italy; (B)INFN Sezione di Perugia, I-06100, Perugia, Italy; (C)University of Perugia, I-06100, Perugia, Italy*
[29] *INFN Sezione di Ferrara, (A)INFN Sezione di Ferrara, I-44122, Ferrara, Italy; (B)University of Ferrara, I-44122, Ferrara, Italy*
[30] *Inner Mongolia University, Hohhot 010021, People's Republic of China*
[31] *Institute of Modern Physics, Lanzhou 730000, People's Republic of China*
[32] *Institute of Physics and Technology, Peace Avenue 54B, Ulaanbaatar 13330, Mongolia*
[33] *Instituto de Alta Investigación, Universidad de Tarapacá, Casilla 7D, Arica 1000000, Chile*
[34] *Jilin University, Changchun 130012, People's Republic of China*
[35] *Johannes Gutenberg University of Mainz, Johann-Joachim-Becher-Weg 45, D-55099 Mainz, Germany*
[36] *Joint Institute for Nuclear Research, 141980 Dubna, Moscow region, Russia*
[37] *Justus-Liebig-Universitaet Giessen, II. Physikalisches Institut, Heinrich-Buff-Ring 16, D-35392 Giessen, Germany*
[38] *Lanzhou University, Lanzhou 730000, People's Republic of China*
[39] *Liaoning Normal University, Dalian 116029, People's Republic of China*

[40] *Liaoning University, Shenyang 110036, People's Republic of China*
[41] *Nanjing Normal University, Nanjing 210023, People's Republic of China*
[42] *Nanjing University, Nanjing 210093, People's Republic of China*
[43] *Nankai University, Tianjin 300071, People's Republic of China*
[44] *National Centre for Nuclear Research, Warsaw 02-093, Poland*
[45] *North China Electric Power University, Beijing 102206, People's Republic of China*
[46] *Peking University, Beijing 100871, People's Republic of China*
[47] *Qufu Normal University, Qufu 273165, People's Republic of China*
[48] *Renmin University of China, Beijing 100872, People's Republic of China*
[49] *Shandong Normal University, Jinan 250014, People's Republic of China*
[50] *Shandong University, Jinan 250100, People's Republic of China*
[51] *Shanghai Jiao Tong University, Shanghai 200240, People's Republic of China*
[52] *Shanxi Normal University, Linfen 041004, People's Republic of China*
[53] *Shanxi University, Taiyuan 030006, People's Republic of China*
[54] *Sichuan University, Chengdu 610064, People's Republic of China*
[55] *Soochow University, Suzhou 215006, People's Republic of China*
[56] *South China Normal University, Guangzhou 510006, People's Republic of China*
[57] *Southeast University, Nanjing 211100, People's Republic of China*
[58] *State Key Laboratory of Particle Detection and Electronics, Beijing 100049, Hefei 230026, People's Republic of China*
[59] *Sun Yat-Sen University, Guangzhou 510275, People's Republic of China*
[60] *Suranaree University of Technology, University Avenue 111, Nakhon Ratchasima 30000, Thailand*
[61] *Tsinghua University, Beijing 100084, People's Republic of China*
[62] *Turkish Accelerator Center Particle Factory Group, (A)Istinye University, 34010, Istanbul, Turkey; (B)Near East University, Nicosia, North Cyprus, 99138, Mersin 10, Turkey*
[63] *University of Chinese Academy of Sciences, Beijing 100049, People's Republic of China*
[64] *University of Groningen, NL-9747 AA Groningen, The Netherlands*
[65] *University of Hawaii, Honolulu, Hawaii 96822, USA*
[66] *University of Jinan, Jinan 250022, People's Republic of China*
[67] *University of Manchester, Oxford Road, Manchester, M13 9PL, United Kingdom*
[68] *University of Muenster, Wilhelm-Klemm-Strasse 9, 48149 Muenster, Germany*
[69] *University of Oxford, Keble Road, Oxford OX13RH, United Kingdom*
[70] *University of Science and Technology Liaoning, Anshan 114051, People's Republic of China*
[71] *University of Science and Technology of China, Hefei 230026, People's Republic of China*
[72] *University of South China, Hengyang 421001, People's Republic of China*
[73] *University of the Punjab, Lahore-54590, Pakistan*
[74] *University of Turin and INFN, (A)University of Turin, I-10125, Turin, Italy; (B)University of Eastern Piedmont, I-15121, Alessandria, Italy; (C)INFN, I-10125, Turin, Italy*
[75] *Uppsala University, Box 516, SE-75120 Uppsala, Sweden*
[76] *Wuhan University, Wuhan 430072, People's Republic of China*
[77] *Yantai University, Yantai 264005, People's Republic of China*
[78] *Yunnan University, Kunming 650500, People's Republic of China*
[79] *Zhejiang University, Hangzhou 310027, People's Republic of China*
[80] *Zhengzhou University, Zhengzhou 450001, People's Republic of China*

[a] *Deceased*
[b] *Also at the Moscow Institute of Physics and Technology, Moscow 141700, Russia*
[c] *Also at the Novosibirsk State University, Novosibirsk, 630090, Russia*
[d] *Also at the NRC "Kurchatov Institute", PNPI, 188300, Gatchina, Russia*
[e] *Also at Goethe University Frankfurt, 60323 Frankfurt am Main, Germany*
[f] *Also at Key Laboratory for Particle Physics, Astrophysics and Cosmology, Ministry of Education; Shanghai Key Laboratory for Particle Physics and Cosmology; Institute of Nuclear and Particle Physics, Shanghai 200240, People's Republic of China*

JHEP05(2024)141

[g] *Also at Key Laboratory of Nuclear Physics and Ion-beam Application (MOE) and Institute of Modern Physics, Fudan University, Shanghai 200443, People's Republic of China*
[h] *Also at State Key Laboratory of Nuclear Physics and Technology, Peking University, Beijing 100871, People's Republic of China*
[i] *Also at School of Physics and Electronics, Hunan University, Changsha 410082, China*
[j] *Also at Guangdong Provincial Key Laboratory of Nuclear Science, Institute of Quantum Matter, South China Normal University, Guangzhou 510006, China*
[k] *Also at MOE Frontiers Science Center for Rare Isotopes, Lanzhou University, Lanzhou 730000, People's Republic of China*
[l] *Also at Lanzhou Center for Theoretical Physics, Lanzhou University, Lanzhou 730000, People's Republic of China*
[m] *Also at the Department of Mathematical Sciences, IBA, Karachi 75270, Pakistan*
[n] *Also at Ecole Polytechnique Federale de Lausanne (EPFL), CH-1015 Lausanne, Switzerland*
[o] *Also at Helmholtz Institute Mainz, Staudinger Weg 18, D-55099 Mainz, Germany*
[p] *Also at School of Physics, Beihang University, Beijing 100191, China*

JHEP05(2024)141